ELSEVIER

Chemical Engineering Journal 135S (2008) S57–S65

Chemical Engineering Journal

www.elsevier.com/locate/cej

Oxidation of organic compounds in a microstructured catalytic reactor

I.Z. Ismagilov [a], E.M. Michurin [a], O.B. Sukhova [a], L.T. Tsykoza [a], E.V. Matus [a], M.A. Kerzhentsev [a], Z.R. Ismagilov [a,*], A.N. Zagoruiko [a], E.V. Rebrov [b], M.H.J.M. de Croon [b], J.C. Schouten [b]

[a] *Boreskov Institute of Catalysis SB RAS, Prospekt Akademika Lavrentieva 5, Novosibirsk 630090, Russia*
[b] *Eindhoven University of Technology, P.O. Box 513, 5600 MB Eindhoven, The Netherlands*

Abstract

A microstructured catalytic reactor for the oxidation of organic compounds has been fabricated from aluminum alloy AlMgSiCu1 (6082 series, Al51st). The catalyst section was assembled of 63 microstructured plates with catalytic coating. In each plate of 416 μm thickness, 45 semi-cylindrical microchannels of 208 μm in radius with a distance in between of 150 μm were electrodischarge machined. A porous alumina layer of 29 ± 1 μm thickness was produced on the plates by anodic oxidation. The resulting coatings were impregnated with an aqueous solution of copper dichromate followed by drying and calcination at 450 °C to produce active catalysts. Kinetics of deep oxidation of organic compounds *n*-butane, ethanol, and isopropanol was studied in the reactor at 150–360 °C and of 1,1-dimethylhydrazine (unsymmetrical dimethylhydrazine, UDMH) at 200–375 °C. Intermediate reaction products in the reactions of alcohols and UDMH oxidation were identified. For UDMH, these are methane, dimethylamine, formaldehyde 1,1-dimethylhydrazone, and 1,2-dimethyldiazene. Nitrogen atoms from the UDMH and N-containing intermediates were shown to convert mainly to N_2. Kinetic parameters of the reactions of *n*-butane and alcohols (rate constants and apparent activation energies) were calculated using kinetic modeling based on a modified method of quickest descent.

Keywords: Microstructured reactor; Electrodischarge machining; Anodic oxidation; Copper chromite; Catalytic combustion; *n*-Butane; Ethanol; Isopropanol; Unsymmetrical dimethylhydrazine; Kinetic modeling

1. Introduction

Since their first appearance in the 1990s, microstructured reactors (microreactors) have found the numerous areas of application in chemical research, development and production due to a number of their advantages compared to conventional reactors, such as miniature dimensions, more precise process control options, higher efficiency and safety [1,2]. One of the examples of processes successfully realized in catalytic microreactors is gas phase oxidation of various compounds, both partial and deep, with such goals as thermal energy production [3,4], generation of H_2 to be further used in the fuel cells and other types of power systems [5,6], purification of air from hazardous volatile organic compounds (VOCs) [7,8], synthesis of valuable chemicals [9,10], etc., as well as kinetic studies of the relevant reaction mechanisms [11–13]. In the latter case, one can rely upon such unique features of microreactors as high uniformity of temperature and concentration profiles among the microchannels, as well as possibility to function in the kinetic rate-controlling regime in wide temperature range [1,2]. Though the mechanisms of gas phase oxidation of several types of compounds in catalytic microreactors have been extensively studied, including hydrogen [11], ammonia [12], carbon monoxide [13], there is still very limited information about the oxidation of organic compounds [14,15].

In this paper, we present results on kinetic testing of a microstructured catalytic reactor with Cu–Cr oxide catalyst supported on anodized aluminum plates, developed for the study of total catalytic oxidation of organic compounds. Model compounds with high heat of combustion, such as *n*-butane ($\Delta H_{c,gas} = -2877.5$ kJ/mol), ethanol ($\Delta H_{c,liq} = -1367.6$ kJ/mol), isopropanol ($\Delta H_{c,liq} = -2006.9$ kJ/mol), and unsymmetrical dimethylhydrazine (UDMH, $\Delta H_{c,liq} = -1978.7$ kJ/mol) were selected for the study, representing different classes of organic compounds—alkanes, alcohols, and hydrazine derivatives. Special attention was paid to UDMH. This compound is a component of the high-energy propellant for liquid-fueled rockets used in Russia, China, and the U.S. UDMH is a highly toxic compound, close to chemical warfare agents according to its effect on biological objects. The

* Corresponding author. Tel.: +7 383 330 62 19; fax: +7 383 339 73 52.
E-mail address: zri@catalysis.ru (Z.R. Ismagilov).

1385-8947/$ – see front matter © 2007 Elsevier B.V. All rights reserved.
doi:10.1016/j.cej.2007.07.036

maximum allowable concentration for UDMH is 0.1 ppm. The U.S. National Institute for Occupational Safety and Health recommends an exposure limit of 0.06 ppm (0.15 mg/m^3) as a ceiling concentration [16]. In Russia the maximum allowable concentration is 0.1 mg/m^3 for working areas and 0.001 mg/m^3 for populated areas [17]. At the moment, there are no specialized industrial facilities for UDMH treatment, as well as no reliable treatment technologies for UDMH, its vapors, and waste containing it, that meet economical and environmental requirements [18]. We believe that for the treatment of hazardous organic compounds microreactor technology using catalytic oxidation is superior to others because of the possibilities, first, to prevent the onset of explosive reaction regimes in microchannels with large surface-to-volume ratios [9,11] and, second, to minimize the occurrence of "hot spots" by using high heat and mass transfer rates and short contact times characteristic for microreactors [12,13]. Furthermore, even if the microreactor fails, small quantity of chemicals released accidentally could be easily contained [1,2].

Microreactor was developed at the Eindhoven University of Technology in several steps using the methods of computational fluid dynamics (CFD) in order to obtain its overall dimensions, first, with the minimal pressure and temperature gradients and, second, with the maximally uniform flow distribution over the inlets of microchannels. The first task was accomplished by using the initially estimated kinetics of *n*-butane oxidation on individual microstructured plates [19]. For the second task, an original type of inlet flow diffuser was developed using the GAMBIT 2.0 and FLUENT 6.1 software [20], also accounting for some earlier diffuser developments [21]. The goal of this paper is to study oxidation kinetics of the above-mentioned organic compounds in the microreactor, with variation of initial concentrations of oxidized compounds and oxygen, gas hourly space velocity (GHSV) and catalyst temperature, and to apply kinetic modeling for the calculation of reaction rate parameters.

2. Experimental

2.1. Microstructured plates

The aluminum alloy AlMgSiCu1 (6082 series, Al51st) was selected as base microreactor material due to its high heat conductivity and the possibility to prepare a strong porous alumina layer by anodic oxidation. For the microreactor fabrication, Al51st plates with a length of 40 mm and a width of 26.62 mm were taken. These plates, being electrodischarge machined (EDM) by the method of "two incisions", provided a surface roughness of microchannel walls (Ra) below 2.0 μm, which was impossible to obtain with pure aluminum. In each plate of 416 μm thickness, 45 semi-cylindrical microchannels of 208 μm in radius with a distance in between of 150 μm were machined [19].

2.2. Coating development

Porous alumina layer was produced by anodic oxidation of the microstructured Al51st alloy plates in 3.5 wt.% oxalic acid solution at 1.0 ± 0.1 °C for 23 h under current-controlled conditions. The produced alumina layer has cylindrical pores with an average diameter of ca. 40 ± 5 nm and a uniform thickness of 29 ± 1 μm. The used method of anodic oxidation is described in detail in [19].

2.3. Catalyst preparation

Method of catalyst preparation was developed and optimized in [19]. Microstructured Al51st alloy plates with the anodic alumina layer were degreased with acetone and calcined at 300 °C. Catalysts were prepared by impregnation of these plates by an aqueous solution of copper dichromate (410 mg/ml) for 20 min. Then, the excess solution was wiped off with filter paper, followed by drying under an IR lamp for 1 h and calcination at 450 °C for 4 h. Characterization of the catalytic coatings by X-ray photoelectron spectroscopy (XPS), electron spectroscopy of diffuse reflectance (ESDR), chemical analysis, and X-ray microprobe analysis showed that the catalyst contains uniformly distributed Cu(II) and Cr(III) oxides having total content of 5 wt.% with respect to the mass of alumina layer [19].

2.4. Microreactor assembling

Microreactor catalyst section is assembled from 63 microstructured plates with catalytic coatings. This section has a size of ca. 27 mm × 34 mm × 40 mm and contains 2835 semi-cylindrical microchannels. Microreactor has inlet section with a specially designed flow diffuser to achieve maximally uniform reaction mixture velocity distribution at the entrance of each microchannel [20,22] and an outlet quench section cooled by water and ethylene glycol to decrease the temperature of gases leaving catalyst section, thus preventing subsequent homogeneous gas phase reactions (Fig. 1).

2.5. Experimental setup

Microreactor is connected to an automatic PC-interfaced experimental setup equipped with the digital mass-flow controllers (Bronkhorst Hi-Tec) for preparation and supply of reaction mixtures and with the temperature controllers. Supply of liquid vapors was performed using saturator with helium as a carrier gas. All the gas lines are placed inside air thermostat heated to 60 °C, where temperature control of all the principal units is provided by a controller "Varta TP 403" and registrator "Oven UKT 38" using chromel–alumel thermocouples with an accuracy of 0.1 °C. Temperature control in the resistively heated microreactor is performed by a controller "West 6100+" and registrator "Voltcraft K204 Datalogger" via another group of chromel–alumel thermocouples, also with an accuracy of 0.1 °C. Prior to each daily experiment, catalyst in the microreactor has undergone oxidative pretreatment cycle for 1 h using approximately the same mixture composition of O_2 and inert gas (N_2 for butane, ethanol, and isopropanol; He for UDMH) as afterwards in the experiment with addition of organic compound to be oxidized, and at the maximal value of temperature to be reached in experiment.

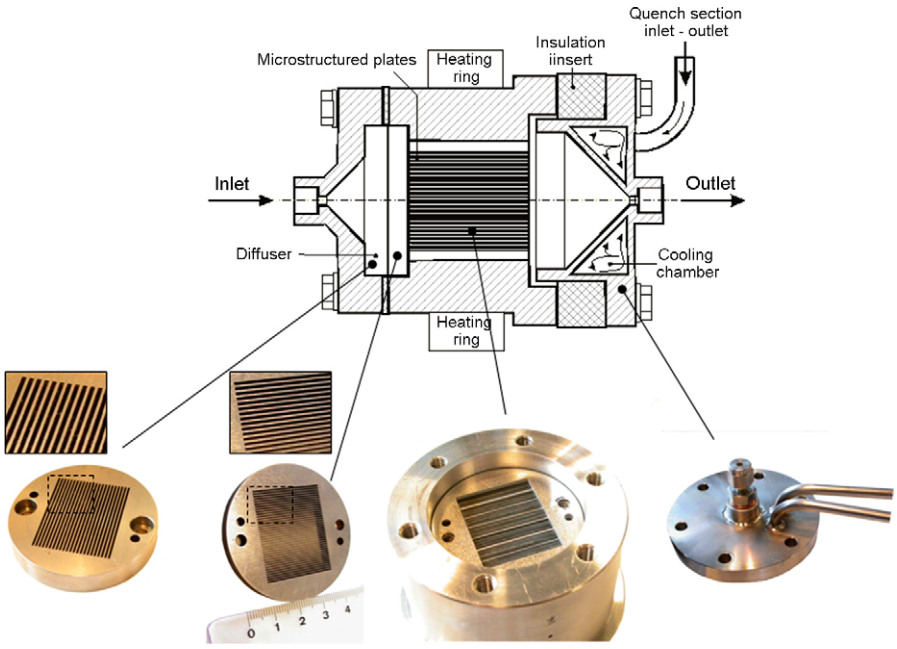

Fig. 1. Cross-section of the catalytic microstructured reactor with photos of its individual parts: vertical and horizontal microchannel sections of inlet flow diffuser, inlet region of microstructured catalytic plates assembled in the housing, quench section with coolant inlet and outlet.

Analysis of the reaction mixtures before and after reactor was performed with a gas chromatograph "Kristall-2000M" equipped with simultaneously operating thermal conductivity detector (TCD) and flame ionization detector (FID).

On the TCD, a stainless steel chromatographic column with diameter of 3 mm and length of 2 m (3 mm × 2 m) with active carbon "SKT" was used for separation and analysis of CO_2 and N_2O. Similar column with NaX molecular sieves was used for the analysis of O_2, N_2, and CO.

For analysis of *n*-butane and alcohols with FID, a stainless steel chromatographic column of 3 mm × 1 m with the sorbent "HayeSep Q-S" was used. Analysis of unsymmetrical dimethylhydrazine and products of its oxidation was performed using a stainless steel column of 2 mm × 3 m with a "Tenax" sorbent.

3. Results and discussions

3.1. *n*-Butane oxidation

Oxidation of *n*-butane with air was studied at initial concentration of 0.2 mmol/l, GHSV in the range of 1600–10,700 h^{-1}, temperature 150–360 °C. The dependencies of *n*-butane conversion on space velocities and temperatures are shown in Fig. 2. Comparison of curves 2 and 3 in Fig. 2 shows that presence of the inlet flow diffuser improves *n*-butane conversion by several % in the whole studied temperature range (example at GHSV = 5360 h^{-1}). This is in qualitative accordance with what is expected based on modeling of such diffuser [20,22] and already tested experimentally in the similar types of microreactors [21]. Oxidation of *n*-butane proceeds with the formation of deep oxidation products CO_2 and H_2O in the whole temperature range (Fig. 3). No products of partial oxidation were detected.

It is known from literature that the Langmuir–Hinshelwood (L–H) type of mechanism is often assumed for the reactions of heterogeneous catalytic oxidation of gaseous organic compounds, such as alkanes, alcohols, and nitrogen-containing ones (see for example [19] and references therein). By applying the L–H approach, the reaction rate order of *n*-butane for its deep catalytic oxidation in the excess of oxygen is close to unity, while for the oxygen this order is close to zero [23,24]. In the case of our microreactor, the observed dependencies of *n*-butane conversion on GHSV (Fig. 2), temperatures (Fig. 3) and initial concentration of oxygen were found to be in agreement with the first and almost zeroth reaction rate orders of *n*-butane and oxygen, respectively, and the rate constants

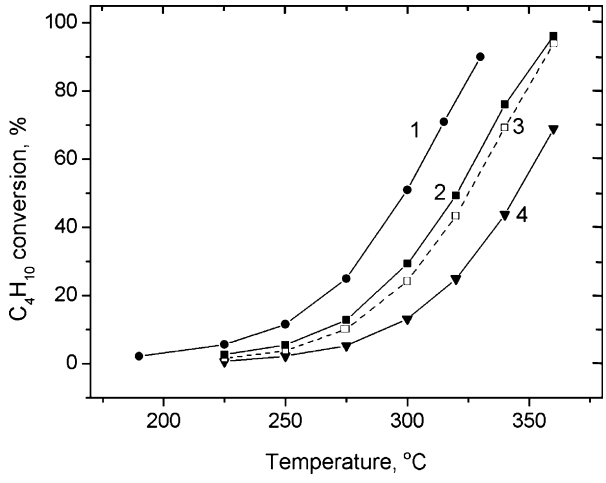

Fig. 2. *n*-Butane conversion vs. temperature upon oxidation with air in the microreactor at initial *n*-butane concentration 0.2 mmol/l and different GHSV values: (1) 1600 h^{-1}, (2) 5360 h^{-1}, (3) 5360 h^{-1} without inlet flow diffuser, (4) 10,700 h^{-1}; GHSV calculated with respect to the volume of catalyst coating.

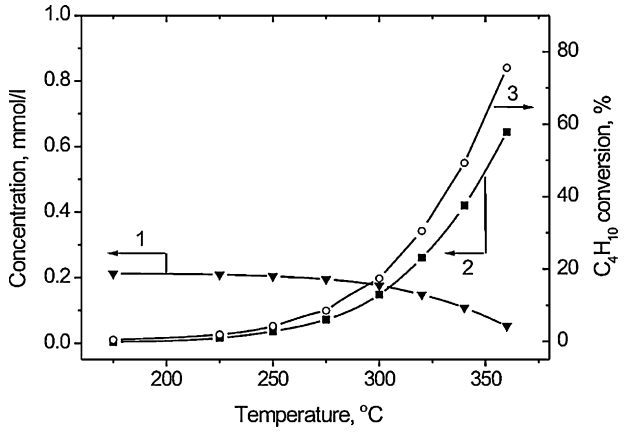

Fig. 3. *n*-Butane concentration (1), CO_2 concentration (2), and *n*-butane conversion (3) vs. temperature upon oxidation in the microreactor with air at initial *n*-butane concentration 0.2 mmol/l and GHSV = 5360 h^{-1}.

k were accordingly calculated using the plug flow approximation.

The Arrhenius plots of calculated dependencies of ln *k* versus 1/*T* for different values of GHSV in the microreactor are shown in Fig. 4 and compared to the one of reference pelletted catalyst 17 wt.%$CuCr_2O_4/Al_2O_3$ with a granule size of 1.0–1.6 mm. The results show that at low temperatures (below 280 °C, on the right-hand side from respective projection on 1/*T* axis) activity of the pelletted catalyst is 1.5–2 times more than that of the microstructured catalyst containing 5 wt.% active component. At higher temperatures the microstructured catalyst exhibits higher efficiency probably due to the absence of diffusion limitations (this is commented further), while the presence of such limitations (internal and external) may affect the reaction rate in case of pelletted catalyst at temperatures above 280 °C. This can be seen in Fig. 4 from the decrease of slope of curve 4 by a factor of 2 on the left-hand side from respective projection on 1/*T* axis. The upper temperature limit for the pelletted catalyst shown in Fig. 4 is 375 °C, and for the microstructured catalyst it is 325 °C. The latter temperature is shown as the limiting one only for the graphical simplicity reasons because, in fact, curves 1–3 hold almost constant slopes (which, in turn, can be interpreted as the continuing absence of diffusion limitations) up to the highest temperature used for *n*-butane oxidation experiments in microreactor, 360 °C (Fig. 3). For the experimental safety reasons, this temperature is approximately 200 °C less than the melting point of Al51st alloy (555 °C) used for microreactor fabrication.

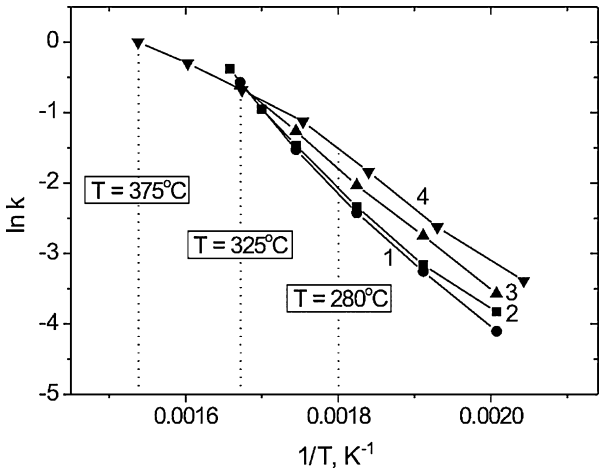

Fig. 4. Temperature dependencies of ln *k* upon *n*-butane oxidation with air at initial *n*-butane concentration 0.2 mmol/l: (1) microreactor, GHSV = 10,700 h^{-1}, (2) microreactor, GHSV = 5360 h^{-1}, (3) microreactor, GHSV = 1600 h^{-1}, (4) pelletted catalyst 17 wt.%$CuCr_2O_4/\gamma$-Al_2O_3, GHSV = 1000 h^{-1}. Projections on 1/*T* axis by dotted lines: temperatures of 280 °C (0.0018 K^{-1}), 325 °C and 375 °C.

Actually, we have shown previously [19] that for the reaction of butane oxidation over pelletted catalyst the Weisz modulus ψ is below 0.1 at 300 °C, indicating the absence of concentration gradients inside granule, but at higher temperatures 350–400 °C this value is over 0.1, which is the evidence that internal diffusion has inhibiting effect on the reaction rate. Calculations show that the value of Weisz modulus remains below 0.1 for the microstructured catalyst at temperatures up to 500 °C, proving that microstructured reactors of this type allow to study intrinsic kinetics in a wide temperature range.

Calculated apparent activation energies of *n*-butane oxidation are within the range of 71–84 kJ/mol, which is close to the literature data [23,24].

3.2. Ethanol oxidation

Ethanol oxidation in the microreactor was studied at ethanol initial concentration in the proximity of 0.45 mmol/l (1 vol.%), oxygen initial concentrations in the range of 4.5–31.2 mmol/l (10–70 vol.%), GHSV in the range of 1600–10,700 h^{-1}, temperature 150–325 °C.

Results of the experiments are shown in Figs. 5–7. At temperatures below 300 °C, the reaction products contain CO_2 and also the products of partial oxidation—acetaldehyde and CO. At higher temperature (325 °C) mainly CO_2 is formed, with concentrations corresponding to the stoichiometry of ethanol deep oxidation. No products of partial oxidation were detected at this temperature (Fig. 5). To verify the results of GC analysis for the reaction mixture of ethanol and its oxidation products, carbon balance data are also included in Fig. 5 for all the temperatures

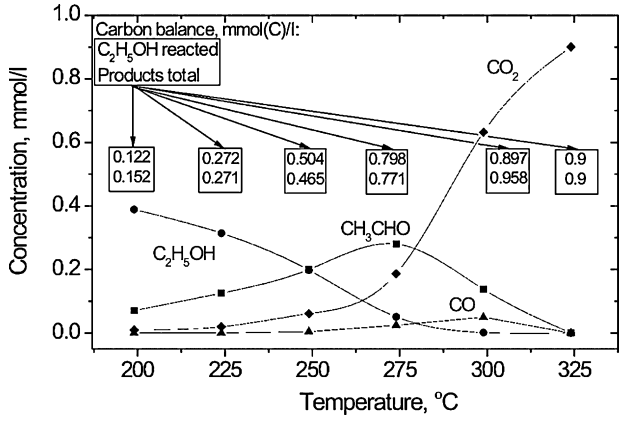

Fig. 5. Temperature dependencies of product concentrations upon ethanol oxidation in the microreactor. Initial concentrations: ethanol 0.45 mmol/l, O_2 8.9 mmol/l (20 vol.%); GHSV = 5360 h^{-1}.

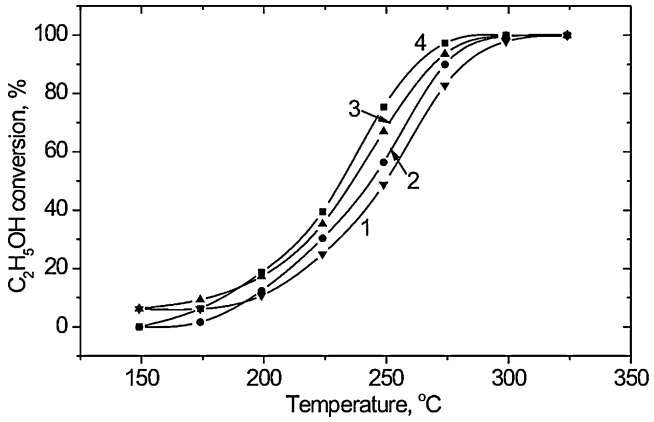

Fig. 6. Temperature dependencies of ethanol conversion upon its oxidation in the microreactor. Initial concentration of ethanol approximately 0.45 mmol/l (1 vol.%). Initial O_2 concentration variable: (1) 4.5 mmol/l (10 vol.%) (ethanol 1.3 vol.%), (2) 8.9 mmol/l (20 vol.%) (ethanol 1.1 vol.%), (3) 22.3 mmol/l (50 vol.%) (ethanol 1.3 vol.%), (4) 31.2 mmol/l (70 vol.%) (ethanol 1.1 vol.%); GHSV = 5360 h^{-1}.

where measurements were made, showing comparison of carbon atom concentrations (mmol/l) in the reacted C_2H_5OH versus total in the products formed (CO_2, CO, and CH_3CHO). Carbon balance appears in overall satisfactory, within relative 10% for all the temperatures except for those around 200 °C. The latter largest deviation can be explained by the uncertainties in GC analysis of products at low concentrations.

Experiments with variation of initial oxygen concentration showed that ethanol conversion increases with oxygen concentration in the medium- and high-temperature range of 200–325 °C (Fig. 6). Some deviations from this general trend are observed in the low-temperature range (150–175 °C), which will be explained further by referring to variations (1.1–1.3 vol.%) in the initial ethanol concentration. Thus, by contrast to *n*-butane, the reaction rate of ethanol oxidation depends both on the concentrations of ethanol and oxygen.

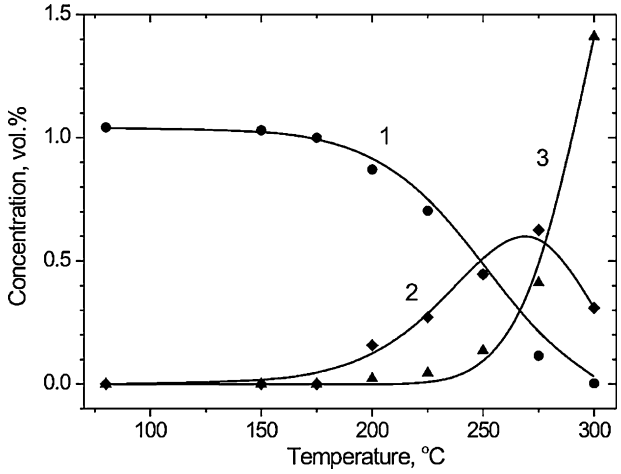

Fig. 7. Composition of reaction products vs. temperature upon ethanol oxidation in the microreactor. Initial concentrations: ethanol 0.45 mmol/l, O_2 8.9 mmol/l (20 vol.%); GHSV = 5360 h^{-1}; (1) ethanol, (2) acetaldehyde, (3) carbon dioxide. The points refer to the experimental data and the lines refer to the results of modeling.

Formation of acetaldehyde as the intermediate reaction product during ethanol oxidation over conventional noble metal and oxide catalysts was as reported previously [25–28]. On the noble metal catalysts Pt/Al_2O_3 [25], Pd/CeO_2–TiO_2 [28], in addition to acetaldehyde, the formation of acetic acid and traces of ethyl acetate and ethylene was observed.

The authors of [26,28] used consecutive reaction schemes for the interpretation of observed results. According to literature, reaction includes the following steps:

$$C_2H_5OH + \tfrac{1}{2}O_2 \rightarrow CH_3CHO + H_2O \quad (1)$$

$$CH_3CHO + \tfrac{5}{2}O_2 \rightarrow 2CO_2 + 2H_2O \quad (2)$$

To obtain formal kinetic equations for the reactions (1) and (2) which would agree with the experimental data, we used software developed at the Boreskov Institute of Catalysis [29], based on a modified method of quickest descent. The quality of experimental data fit for every tested hypothetic kinetic model was estimated by two parameters—the mean absolute deviation of concentrations and the relative confidence interval for model parameters. Criterion of the correctness of obtained results is the invariability of values of the reaction constants for different experimental series.

Based on the analysis of experimental data and on the assumption of consecutive mechanism ((1) and (2)), we suggest the following kinetic model:

$$W_1 = k_1 C_{C_2H_5OH} C_{O_2}^N \quad (3)$$

$$W_2 = k_2 C_{CH_3CHO} C_{O_2}^M \quad (4)$$

where W_i ($i = 1, 2$) are the reaction rates, k_i the apparent rate constants including the product of pre-exponent and activation energy terms $k_i = k_{0,i} \exp(-E_i/RT)$, C_j the steady-state concentration of reagent j in the gas phase, M and N are the reaction rate orders by oxygen.

Our calculations showed that the reaction rate orders with respect to ethanol and acetaldehyde were close to unity. As the first step, model with the first orders with respect to oxygen (M and N) was proposed (Model 1 in Table 1), but the data fit quality appeared to be only moderately good.

Much better results were obtained with Model 2, where reaction orders with respect to oxygen were set as model parameters to be defined. It was shown that the best fit with experimental results was found for Model 2 at values $N = 0.4$ and $M = 0.8$. However, we also tried Model 3 with fixed orders of 0.5 and 1, respectively. Fitting quality in this case was only slightly worse than that for Model 2, but Model 3 seems to be more physically sound because it is more suited to the logic of mass action law and therefore it should be preferred. No special analysis of inter-correlation between kinetic constants was performed, though, to our experience, in case of good quality of solution (low values of relative confidence interval, as it is seen in Table 1) the role of such inter-correlation is not dramatic anyway. All available data points were used simultaneously for the parameter fit. In the given case, when all experimental data belong to similar type of experiments, such approach is reasonable.

Table 1
Kinetic parameters for reaction of ethanol oxidation

Model	$k_{0,1}$ (s^{-1})	$k_{0,2}$ (s^{-1})	E_1 (kJ/mol)	E_2 (kJ/mol)
1	$(9.64 \pm 1.8) \times 10^9$	$(1.48 \pm 0.19) \times 10^{14}$	92.2 ± 1.6	143.5 ± 1.1
2	$(8.56 \pm 0.06) \times 10^7$	$(9.61 \pm 0.69) \times 10^{13}$	75.8 ± 0.6	142.3 ± 0.8
3	$(2.06 \pm 0.2) \times 10^8$	$(3.33 \pm 0.4) \times 10^{15}$	79.1 ± 0.8	157.7 ± 1.0

Model	N_{O_2}	M_{O_2}	Mean absolute deviation of concentrations (%)	Mean relative confidence interval for model parameters (%)
1	1	1	0.064	1.25
2	0.41 ± 0.04	0.82 ± 0.03	0.044	5.07
3	0.5	1	0.047	0.83

The earlier mentioned behavior of ethanol conversion curves in the low-temperature range of Fig. 6 can be explained by the dominating effect of reaction step (1) described by Eq. (3) where, due to the low conversion, steady-state concentration of ethanol is high, close to initial one in the proximity of 1 vol.% (compare with Fig. 5). For the curves 1 and 3, initial concentration of ethanol is 1.3 vol.%, while for the curves 2 and 4, it is 1.1 vol.%, and thus curves 1 and 3 show higher conversion than curves 2 and 4 because of the higher reaction rates for curves 1 and 3, according to the mass action law principle in Eq. (3). Also, based on Eq. (3) applied in the low-temperature range, variation of the initial oxygen concentration seems to make only minor contribution to the ethanol conversion, which can be explained by lower reaction rate order of oxygen compared to ethanol, as well as by low activity of the catalyst at these temperatures. Following the same logic, in the medium- and high-temperature range of Fig. 6, where the steady-state concentration of ethanol is decreasing and the one of acetaldehyde is increasing with a maximum at 275 °C (Fig. 5), conversion of ethanol shows correlation with initial oxygen concentration, according to step (2) described by Eq. (4), where the reaction rate order of oxygen is close to the one of acetaldehyde.

Fig. 7 illustrates good correspondence of the experimental and above outlined Model 3 data which can be used for engineering design of the microreactor. It should be noted that this model represents only a simplified reaction scheme and not the detailed gas-surface mechanism, which will require more experimental data.

3.3. Isopropanol oxidation

Isopropanol oxidation in the microreactor was studied at isopropanol initial concentration of 0.45 mmol/l, oxygen initial concentration in the range of 4.5–31.2 mmol/l (10–70 vol.%), GHSV in the range of 1600–10,700 h^{-1}, temperature 175–325 °C.

Oxidation of isopropanol at $T < 325$ °C proceeds also with formation of the intermediate products of partial oxidation—acetone and CO. In addition, a parallel reaction of isopropanol dehydration with propylene formation takes place (Fig. 8). At $T > 325$ °C mainly the products of deep oxidation—CO_2 and H_2O are formed.

These results agree with literature data [30,31]. The authors of [30] studied chemisorption, decomposition, and oxidation of isopropanol on pure metal oxide catalysts. It was shown that all the catalysts with the exception of Fe_2O_3 and TiO_2 exhibited extremely high selectivity at low temperatures (200 °C) to either RedOx or acidic reaction route products. Redox surface sites yield acetone and acidic surface sites yield propylene. According to [30], Cu(II) and Cr(III) oxides in the microstructured catalyst should be responsible for the acetone formation and acidic sites on the alumina support should catalyze the reaction of isopropanol dehydration with the formation of propylene. At higher temperatures, these products are oxidized with the formation of CO_2 and water.

Literature data and our experimental results allow to propose the following overall simplified reaction scheme for isopropanol oxidation:

$$C_3H_7OH \rightarrow C_3H_6 + H_2O \quad (5)$$

$$C_3H_7OH + \tfrac{1}{2}O_2 \rightarrow C_3H_6O + H_2O \quad (6)$$

$$C_3H_6 + \tfrac{9}{2}O_2 \rightarrow 3CO_2 + 3H_2O \quad (7)$$

$$C_3H_6O + 4O_2 \rightarrow 3CO_2 + 3H_2O \quad (8)$$

In this scheme, neglecting the small amounts of CO formed, we assume that isopropanol is consumed in the parallel reaction of formation of two intermediates—acetone and propylene, which are further oxidized to CO_2 and water. Based on the approach similar to one used above for modeling ethanol oxida-

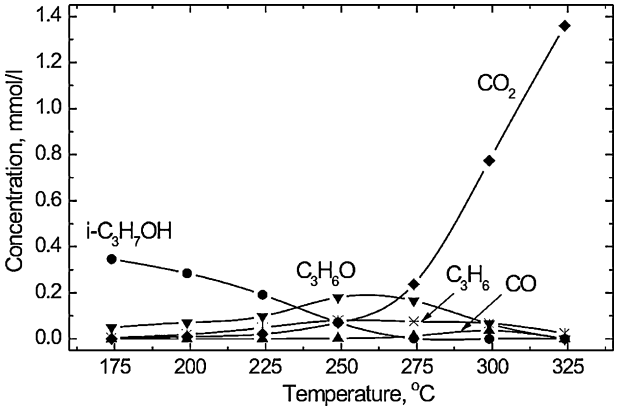

Fig. 8. Temperature dependencies of product concentrations upon isopropanol oxidation in the microreactor. Initial concentrations: isopropanol 0.35 mmol/l, O_2 8.9 mmol/l (20 vol.%); GHSV = 5360 h^{-1}.

Table 2
Kinetic parameters for reaction of isopropanol oxidation

$k_{0,1}$ ($\times 10^7$ s^{-1})	8.32 ± 1.35
$k_{0,2}$ ($\times 10^7$ s^{-1})	4.58 ± 0.07
$k_{0,3}$ ($\times 10^9$ s^{-1})	6.75 ± 1.47
$k_{0,4}$ ($\times 10^{20}$ s^{-1})	1.39 ± 0.32
E_1 (kJ/mol)	81.1 ± 1.4
E_2 (kJ/mol)	71.6 ± 1.4
E_3 (kJ/mol)	95.7 ± 1.8
E_4 (kJ/mol)	210.3 ± 2.1

tion, the following rate equations are proposed:

$$W_1 = k_1 C_{C_3H_7OH} \quad (9)$$

$$W_2 = k_2 C_{C_3H_7OH} C_{O_2}^{0.5} \quad (10)$$

$$W_3 = k_3 C_{C_3H_6} C_{O_2} \quad (11)$$

$$W_4 = k_4 C_{C_3H_6O} C_{O_2} \quad (12)$$

where W_i ($i = 1, 2, 3, 4$) are the reaction rates, k_i the apparent rate constants including the product of pre-exponent and activation energy terms $k_i = k_{0,i} \exp(-E_i/RT)$, C_j is the steady-state concentration of reagent j in the gas phase, the reaction rate orders by oxygen are either 0, 0.5 or 1.

The calculated kinetic parameters for one of the isopropanol oxidation models are given in Table 2. Good correspondence of the modeling and experimental data is illustrated by Fig. 9 (mean deviation of calculated and experimental data was equal to 0.065%, relative confidence interval for the model parameters—1.6%). As in the case of ethanol, it should be noted that these results can be used for the calculation of concentrations of isopropanol oxidation products under different conditions in the microreactor with Cu–Cr oxide catalyst.

3.4. Unsymmetrical dimethylhydrazine oxidation

Unsymmetrical dimethylhydrazine (UDMH) oxidation in the microreactor was studied at an UDMH initial concentration of 0.16–0.4 mmol/l, oxygen initial concentration in the range 8.9–31.2 mmol/l (20–70 vol.%), GHSV in the range of 5360–10,700 h^{-1}, temperature 200–375 °C. UDMH vapors were supplied from the saturator with a helium flow and diluted with helium and oxygen in the mixer to form initial reaction mixtures. Helium was chosen for the reason to measure concentrations of nitrogen formed from UDMH.

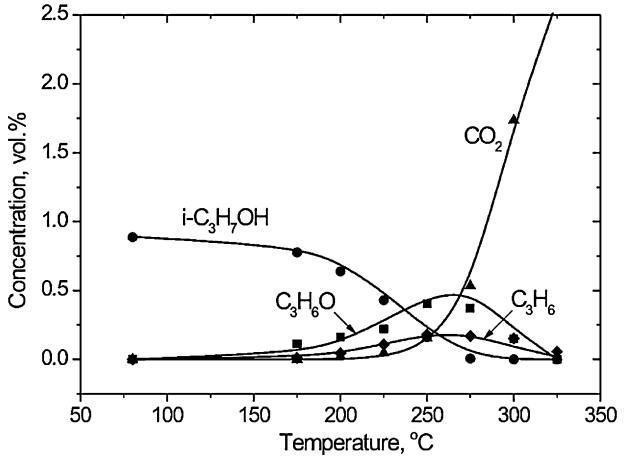

Fig. 9. Composition of reaction products vs. temperature upon isopropanol oxidation in the microreactor. Initial concentrations: isopropanol 0.35 mmol/l, O_2 8.9 mmol/l (20 vol.%); GHSV = 5360 h^{-1}. The points refer to the experimental data and the lines refer to the results of modeling.

Table 3
Concentrations of products of UDMH oxidation (C_j) and total concentrations of carbon ($C_{\Sigma C}$) and nitrogen ($C_{\Sigma N}$) (mmol/l) at different temperatures

T (°C)	C_{CH_4}	C_{DMA}	C_{DDA}	C_{MDMH}	C_{CO_2}	C_{N_2}	$C_{\Sigma C}$	$C_{\Sigma N}$
200	0.0039	0.12	0.03	0.16	0.028	0.11	0.652	0.720
240	0.002	0.156	0.03	0.09	0.045	0.12	0.599	0.636
260	0.002	0.014	0.12	0.10	0.063	0.14	0.533	0.734
300	0.0005	0.0007	0.16	0.02	0.18	0.17	0.541	0.701

Initial concentrations: UDMH 0.4 mmol/l, O_2 8.9 mmol/l (20 vol.%); GHSV = 5360 h^{-1}.

First experiments which were performed at UDMH initial concentration of 0.4 mmol/l, oxygen initial concentration 8.9 mmol/l (20 vol.%), GHSV = 5360 h^{-1}, and temperature in the range of 200–300 °C, showed that UDMH is completely converted to oxidation products already at 200 °C, where its residual concentration was below 0.001 mmol/l. Oxidation products contain CH_4, dimethylamine $(CH_3)_2NH$—DMA, 1,2-dimethyldiazene CH_3–N=N–CH_3—DDA, formaldehyde dimethylhydrazone $(CH_3)_2N$–N=CH_2 (alias methylenedimethylhydrazine—MDMH), CO_2 and nitrogen. Composition of the reaction products is similar to that observed in [32–34] for UDMH oxidation by air over pelletted catalysts. At the temperature of 300 °C only 23% of UDMH was converted to CO_2. Mass balance shows that about 20–30% of carbon and 10–20% of nitrogen should be in the form of some unidentified products (Table 3). Actually, it was found that in addition to the above-listed products, formation of the yellow resinous matter took place, which was deposited in the reactor outlet section and in the outlet tube, eventually blocking the gas passage. This resin could be easily removed by washing with ethanol.

Further experiments were performed at lower UDMH initial concentration (0.16 and 0.3 mmol/l), at higher oxygen initial concentration (9.7 and 34.8 mmol/l (21.7 and 78 vol.%)) and in temperature range extended to 375 °C to reduce formation of the resin. Results of the experiments are given in Figs. 10 and 11.

Results show that at higher temperatures (350–375 °C) the dominating products formed from UDMH are CO_2, N_2 and N_2O (corresponding amounts of H_2O were not analyzed). Small amounts of methane (ca. 0.01 mmol/l) were also detected. Mass balance of carbon and nitrogen is within the accuracy of GC analysis and corresponds to practically total oxidation of UDMH to CO_2. The formed methane is a rather stable compound and its complete oxidation is expected to take place at temperatures over 400 °C. Nitrogen in UDMH is transformed mainly to N_2 with a selectivity of 90% and to N_2O with a selectivity of 10%.

These results generally agree with those previously obtained in experiments performed with a pelletted catalyst of an analogous composition 20 wt.%$Cu_xMg_{1-x}Cr_2O_4/\gamma$-$Al_2O_3$ [32–34].

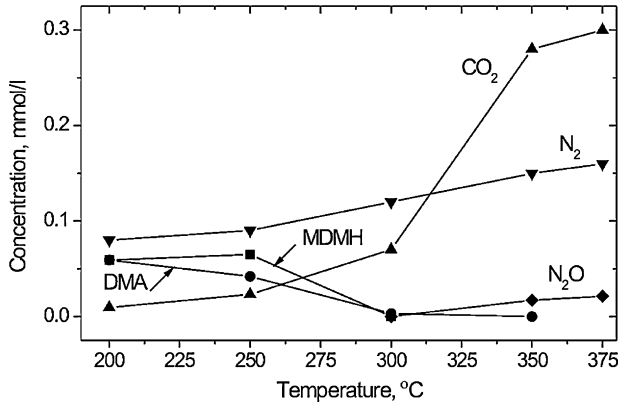

Fig. 10. Temperature dependencies of concentrations of UDMH oxidation products in the microreactor. Initial concentrations: UDMH 0.16 mmol/l in He–O_2 mixture, O_2 9.7 mmol/l (21.7 vol.%); GHSV = 11570 h^{-1}.

Similarly, practically complete UDMH conversion to CO_2 and N_2 was attained over the pelletted catalyst at temperatures over 300 °C and comparable amounts of N_2O and CH_4 were found in the reaction products.

Methane, MDMH, DMA, and DDA are present in the reaction products in wide temperature range. They are already formed in significant quantities at 200 °C. Based on the presence of these compounds at the reactor outlet, and the previous results [32–34], it is possible to suggest a probable L–H type reaction scheme of UDMH heterogeneous catalytic oxidation, proceeding via the following steps:

$$(CH_3)_2N\text{–}NH_2 + [] \rightarrow [(CH_3)_2N\text{–}NH_2]_{ads} \quad (13)$$

$$[(CH_3)_2N\text{–}NH_2]_{ads} + [O]_{ads} \rightarrow [(CH_3)_2N{=}N]_{ads} + [H_2O]_{ads} \quad (14)$$

$$[(CH_3)_2N{=}N]_{ads} + [(CH_3)_2N{=}N]_{ads} \rightarrow [(CH_3)_2N\text{–}N{=}CH_2]_{ads} + [CH_3N{=}NH]_{ads} \quad (15)$$

$$[(CH_3)_2N\text{–}N{=}CH_2]_{ads} \rightarrow CH_3\text{–}N{=}N\text{–}CH_3 + [CH_2]_{ads} \quad (16)$$

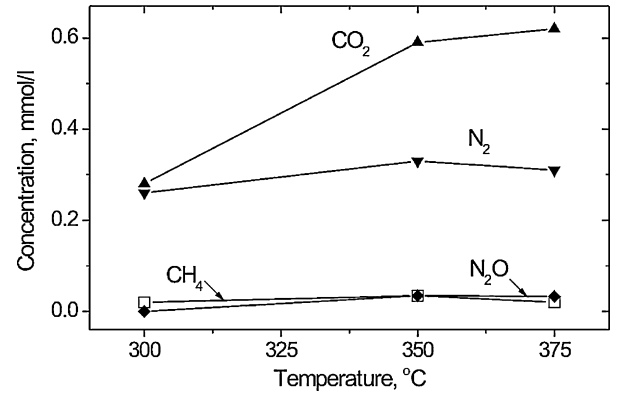

Fig. 11. Temperature dependencies of concentrations of UDMH oxidation products in the microreactor. Initial concentrations: UDMH 0.3 mmol/l in He–O_2 mixture, O_2 34.8 mmol/l (78 vol.%); GHSV = 5360 h^{-1}.

$$[(CH_3)_2N\text{–}N{=}CH_2]_{ads} \rightarrow (CH_3)_2N\text{–}N{=}CH_2 + [] \quad (17)$$

$$4[(CH_3)_2N\text{–}N{=}CH_2]_{ads} + 11[O]_{ads} \rightarrow 4(CH_3)_2NH + 4CO_2 + 2H_2O + N_2 + N_2O + 15[] \quad (18)$$

$$[CH_3N{=}NH]_{ads} \rightarrow CH_4 + N_2 + [] \quad (19)$$

$$2[CH_3N{=}NH]_{ads} + 9[O]_{ads} \rightarrow 2CO_2 + 4H_2O + N_2 + N_2O + 11[] \quad (20)$$

where [ ] denotes the active site of catalyst.

The proof of this mechanism and its elucidation still requires additional research.

4. Conclusions

Kinetics of deep oxidation of organic compounds (*n*-butane, ethanol, and isopropanol) was studied in a microstructured reactor with Cu–Cr oxide catalyst in the temperature range of 150–360 °C. Intermediate reaction products in the reactions of alcohols oxidation were identified and reaction schemes were proposed. Kinetic parameters of the reactions (rate constants and apparent activation energies) were estimated using kinetic modeling based on a modified method of quickest descent.

Kinetic studies of oxidation of unsymmetrical dimethylhydrazine (UDMH) were performed in the temperature range of 200–375 °C. Intermediate reaction products were identified (methane, dimethylamine, formaldehyde 1,1-dimethylhydrazone, and 1,2-dimethyldiazene) and a probable reaction scheme was proposed. UDMH was shown to convert mainly to N-containing organic compounds at temperatures below 300 °C, but mainly to CO_2, H_2O, and N_2 at higher temperatures of 350–375 °C. In summary, this work provides one of illustrative examples how the microreactors can be successfully used for catalytic oxidation of organic compounds, which can be applied for energy production, safe and efficient abatement of hazardous VOCs, as well as for kinetic studies of these reactions.

Acknowledgments

The joint support of this work by the Netherlands Organization for Scientific Research (NWO) and Russian Foundation for Basic Research (RFBR) in the frame of Project 047.15.007. is gratefully acknowledged.

References

[1] G. Kolb, V. Hessel, Chem. Eng. J. 98 (2004) 1–38.
[2] L. Kiwi-Minsker, A. Renken, Catal. Today 110 (2005) 2–14.
[3] K. Schubert, J. Brandner, M. Fichtner, G. Linder, U. Schugulla, A. Wenka, Microscale Thermophys. Eng. 5 (2001) 17–39.
[4] J. Vican, B.F. Gajdeczko, F.L. Dryer, D.L. Milius, I.A. Aksay, R.A. Yetter, Proc. Combust. Inst. 29 (2002) 909–916.
[5] A.Y. Tonkovich, S. Perry, Y. Wang, D. Qiu, T. LaPlante, W.A. Rogers, Chem. Eng. Sci. 59 (2004) 4819–4824.

[6] G.-G. Park, S.-D. Yim, Y.-G. Yoon, C.-S. Kim, D.-J. Seo, K. Eguchi, Catal. Today 110 (2005) 108–113.
[7] I. Yuranov, N. Dunand, L. Kiwi-Minsker, A. Renken, Appl. Catal. B 36 (2002) 183–191.
[8] J. Łojewska, A. Kołodziej, P. Dynarowicz-Łątka, A. Wesełucha-Birczyńska, Catal. Today 101 (2005) 81–91.
[9] Y.S.S. Wan, A. Gavrilidis, K.L. Yeung, Trans. IChemE A 81 (2003) 1–7.
[10] S. Walter, S. Malmberg, B. Schmidt, M.A. Liauw, Chem. Eng. Res. Des. A 83 (2005) 1019–1029.
[11] M.T. Janicke, H. Kestenbaum, U. Hagendorf, F. Schüth, M. Fichtner, K. Schubert, J. Catal. 191 (2000) 282–293.
[12] E.V. Rebrov, S.A. Duinkerke, M.H.J.M. de Croon, J.C. Schouten, Chem. Eng. J. 93 (2003) 201–216.
[13] S.K. Ajmera, C. Delattre, M.A. Schmidt, K.F. Jensen, J. Catal. 209 (2002) 401–412.
[14] Y. Suzuki, J. Saito, N. Kasagi, Jpn. Soc. Mech. Eng. Int. J. B 3 (2004) 522–527.
[15] R.M. Tiggelaar, P.W.H. Loeters, P. van Male, R.E. Oosterbroek, J.G.E. Gardeniers, M.H.J.M. de Croon, J.C. Schouten, M.C. Elwenspoek, A. van den Berg, Sens. Actuators 112 (2004) 77.
[16] U.S. Department of Labor, Occupational Safety & Health Administration, Chemical Sampling Information, 1,1-dimethylhydrazine, http://www.osha.gov/dts/chemicalsampling/data/CH_236300.html.
[17] Chemical Search Engine, 1,1-dimethylhydrazine, http://www.chemindustry.com/apps/search?search_term=unsymmetrical-Dimethylhydrazine.
[18] E.W. Schmidt, Hydrazine and Its Derivatives: Preparation, Properties and Applications, 2nd ed., Wiley, New York, 2001.
[19] I.Z. Ismagilov, R.P. Ekatpure, L.T. Tsykoza, E.V. Matus, E.V. Rebrov, M.H.J.M. de Croon, M.A. Kerzhentsev, J.C. Schouten, Catal. Today 105 (2005) 516–528.
[20] M.J.M. Mies, E.V. Rebrov, M.H.J.M. de Croon, J.C. Schouten, I.Z. Ismagilov, Inlet section for micro-reactor, Dutch Patent P6001475PCT (2005).
[21] M.J.M. Mies, E.V. Rebrov, M.H.J.M. de Croon, J.C. Schouten, Chem. Eng. J. 101 (2004) 225–235.
[22] I.Z. Ismagilov, R.P. Ekatpure, E.V. Rebrov, M.H.J.M. de Croon, J.C. Schouten, AIChE J. 53 (2007) 28–38.
[23] Z.R. Ismagilov, O.Yu. Podyacheva, M.A. Kerzhentsev, V.N. Bibin, A. Ermakova, G.K. Chermashentseva, Kinetika i Kataliz 29 (1988) 254 (in Russian).
[24] M. Aryafar, F. Zaera, Catal. Lett. 48 (1997) 173–183.
[25] Z.R. Ismagilov, N.M. Dobrynkin, V.V. Popovskii, React. Kinet. Catal. Lett. 10 (1979) 55–59.
[26] Z.R. Ismagilov, V.N. Bibin, V.V. Popovskii, N.M. Dobrynkin, React. Kinet. Catal. Lett. 23 (1983) 143–147.
[27] P. Larsson, A. Andersson, Appl. Catal. B 24 (2000) 175–192.
[28] R. Lin, M. Luo, Q. Xin, G. Sun, Catal. Lett. 93 (2004) 139–144.
[29] V.N. Tomilov, A.N. Zagoruiko, P.A. Kuznetsov, Proceedings of the 3rd International Conference on "Unsteady State Processes in Catalysis", St. Petersburg, Russia, June 30–July 3, 1998, pp. 172–173.
[30] D. Kulkarni, I.E. Wachs, Appl. Catal. A 237 (2002) 121–137.
[31] L. Gambaro, J. Mol. Catal. A 247 (2006) 31–35.
[32] Z.R. Ismagilov, M.A. Kerzhentsev, I.Z. Ismagilov, V.A. Sazonov, V.N. Parmon, G.L. Elizarova, O.P. Pestunova, V.A. Shandakov, Yu.L. Zuev, V.N. Eryomin, N.V. Pestereva, F. Garin, H.J. Veringa, Catal. Today 75 (2002) 277–285.
[33] I.Z. Ismagilov, V.V. Kuznetsov, A.P. Nemudryi, O.Yu. Podyacheva, Kinet. Catal. 45 (2004) 722–729.
[34] I.Z. Ismagilov, M.A. Kerzhentsev, V.A. Rogov, V.A. Shandakov, Proceedings of the Russian National Conference on "Utilization of Solid Propellant Rocket Engines. Problems and Methodology of Utilization of Composite Solid Rocket Propellants, Waste of Specialized Production and Residues of Liquid Rocket Propellants in the Elements of Rocket and Space Equipment", Federal Research and Production Center "Altai", Biysk, Russia, September 25–28, 2001, pp. 67–74 (in Russian).